UCRL-JC-133403
PREPRINT

A Micromechanics Model of the Elastic Properties of Human Dentin

J.H. Kinney
M. Balooch
G.W. Marshall
S.J. Marshall

This paper was prepared for submittal to
Archives of Oral Biology

February 18, 1999

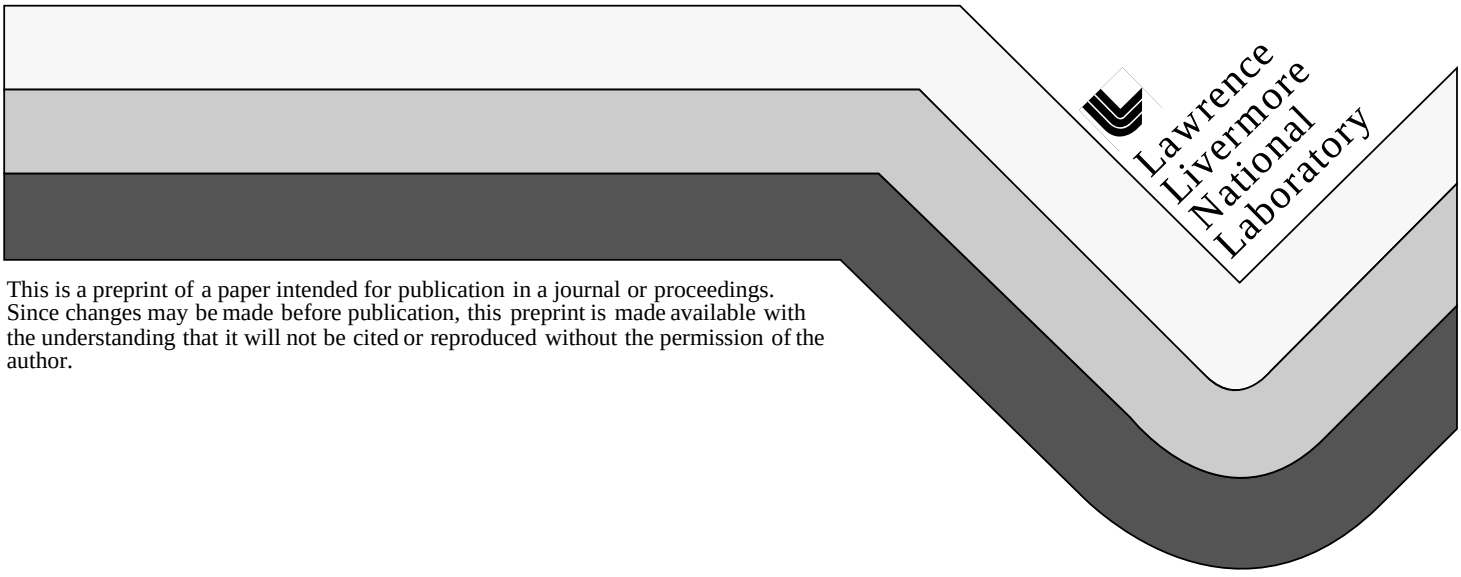

A Micromechanics Model of the Elastic Properties of Human Dentin

J.H. Kinney, M. Balooch, G.W. Marshall*, and S.J. Marshall*
Department of Chemistry and Materials Science
Lawrence Livermore National Laboratory
Livermore, CA

* Department of Restorative Dentistry
University of California, San Francisco

submitted to Archives of Oral Biology

corresponding author:

John H. Kinney, Ph.D.
Department of Chemistry and Materials Science
L–350; P.O. Box 808
Lawrence Livermore National Laboratory
Livermore, CA 94550
Telephone: 925–422–6669
Fax: 925–736–6889
Email: jhkinney@llnl.gov

Keywords: dentin, micromechanics, mechanical properties, atomic force microscopy, indentation, Young's modulus, shear modulus.

Running title: Micromechanics of Dentin

Funding Source: U.S. National Institutes of Health, NIDCR grant number PO1DE09859

Abstract

A generalized self-consistent model of cylindrical inclusions in a homogeneous and isotropic matrix phase was used to study the effects of tubule orientation on the elastic properties of dentin. Closed form expressions for the five independent elastic constants of dentin were derived in terms of tubule concentration, and the Young's moduli and Poisson ratios of peri– and intertubular dentin. An atomic force microscope (AFM) indentation technique determined the Young's moduli of the peri– and intertubular dentin as approximately 30 GPa and 15 GPa, respectively. Over the natural variation in tubule density found in dentin, there was only a slight variation in the axial and transverse shear moduli with position in the tooth, and there was no measurable effect of tubule orientation. We conclude that tubule orientation has no appreciable effect on the elastic behavior of normal dentin, and that the elastic properties of healthy dentin can be modeled as an isotropic continuum with a Young's modulus of approximately 16 GPa and a shear modulus of 6.2 GPa.

Introduction

Dentin, the mineralized tissue forming the bulk of the tooth, lies between the enamel and the pulp chamber. It has a characteristic microstructure consisting of a hydrated matrix of type I collagen that is reinforced with a nanocrystalline carbonated apatite. This matrix phase lies between nearly cylindrical tubules that run from the dentin-enamel junction to the pulp chamber. The tubules are the pathways of the formative odontoblast cells and, as they move inward during formation of the crown, the tubule numerical density increases 2-4 times with depth [Marshall, 1993]. The tubule lumens, which are roughly 1 μm in diameter, are surrounded or lined by a hypermineralized cylinder of peritubular dentin composed largely of apatite that is also roughly 0.5- 1.5 μm in thickness. The formation of the peritubular dentin occurs after mineralization of the matrix, and may be formed as a passive precipitation rather than as an active part of the mineralization process [Ten Cate, 1994]. It has not been established if the peritubular dentin serves any role in enhancing the mechanical properties of dentin tissue.

The elastic properties of dentin are of considerable importance for understanding the mechanical properties of calcified tissue in general, and for understanding alterations in the mechanical response of such tissues as determined by disease and age. In addition it is important to understand the elastic response of dentin to external loading, as this has important implications for understanding masticatory loading effects, the effect of microstructural alterations due to caries, sclerosis, and aging, as well as understanding the effects of the wide variety of restorative dental procedures that range from preparation design to bonding methods.

In spite of its importance, there is great inconsistency with the reported values of the Young's modulus of dentin. Measurements of the Young's modulus span a range from about 10 to 20 GPa, a range that appears to be independent of testing method (see Table 1). Furthermore, it is interesting to note that despite marked advances in both our theoretical understanding of the mechanics of composite structures and improved testing methods, the

large discrepancies in measured values of the elastic modulus persist, as demonstrated by two recently published papers that report values of 20.3 and 8.7–11.2 GPa, respectively [Xu, et al. 1998; Merideth, et al. 1996].

The large discrepancy in the elastic modulus of dentin reflects the difficulties in performing mechanical tests on small specimens. It is also true that measurements can be affected by variations in specimen wetness, possible variations in mineralization, and tubule density and orientation. Clearly, an accurate determination of the elastic properties of dentin would benefit from a model that accounts for tissue variability in terms of a limited number of properties that can be accurately measured.

Dentin can be analyzed at many length scale hierarchies. At the microscopic level, dentin can be studied as an aggregate of mineral and collagen. At the microstructural level, dentin is composed of cylindrical tubules interpenetrating a partially mineralized matrix phase of type I collagen. Finally, at the functional, or continuum level, dentin looks like a homogeneous substance that fills the space between the enamel and the pulp. Previous attempts to model the elastic properties of dentin have focused on the constituent materials properties at the microscopic level, and have relied on bounding principals such as Voigt and Reuss or Hashin-Shtrikman [Katz, 1971]. In bounding models, the elastic behavior of dentin is determined only by the relative volume fractions of the collagen and mineral phases. For dentin, however, these models have proved to be of little value because the elastic properties of the two constituent phases differ by several orders of magnitude. About the only use for bounds is as a check on the validity of any other theoretical model: the Young's modulus of healthy dentin cannot exceed 40 GPa, nor be less than about 5 GPa. Such wide bounds do not help with the assessment of the reliability of the experimental measurements, since most reported measurements lie within these upper and lower bounds.

Christensen and Lo [summarized in Christensen 1990] have developed a micromechanics model of cylindrical inclusions in a homogeneous matrix phase. This

model is quite powerful in that it covers the complete range of possible inclusion densities, and presents simple analytical expressions for the elastic constants. The purpose of this paper is to extend this model to dentin. The model requires two measurements: the Young's modulus of the matrix phase (intertubular dentin) and the modulus of the cylindrical inclusion (the tubule lumen with its surrounding peritubular cuff). We report the values for these moduli based on atomic force microscope (AFM) indentation of fully hydrated specimens, and use them to predict the continuum elastic properties of dentin. We then use the model to test the hypothesis that the elastic properties of dentin are dominated by the matrix, and that the dentinal tubules contribute only slightly to the mechanical properties.

Materials and Methods

micromechanics model

The micromechanics model of dentin proposed here is a straightforward extension of the generalized self–consistent formalism, also called the three–phase model, of cylindrical inclusions in a uniform matrix phase that was pioneered by Christensen and Lo [Christensen 1990]. In the original presentation, both the matrix phase and the material comprising the cylindrical inclusion were assumed isotropic. Transverse anisotropy of the composite structure was imposed by the parallel alignment of the cylindrical inclusions. A boundary value problem was formulated by embedding a cylindrical inclusion into the matrix, with the areal fractions adjusted to account for the correct concentration of the inclusions. This two phase model was then embedded in an effective medium that matched the continuum properties of the bulk composite. With this model, analytic solutions for the five independent elastic constants were obtained without restrictions on the concentration or symmetry of the cylindrical inclusions.

The axial Young's modulus was derived as a function of the concentration (areal fraction of the inclusions crossing the plane normal to their orientation, c) of the inclusions, the Young's moduli of the matrix (E_m) and cylindrical inclusion (E_f), and a factor, γ, that depends upon the difference in Poisson ratio between the two phases [Christensen 1990]:

$$E_{11} = cE_f + (1-c)E_m + \gamma\left(c, \nu_f, \nu_m, \mu_f, \mu_m, \kappa_f, \kappa_m\right) \qquad (1)$$

In this formalism, ν_f, ν_m, μ_f, μ_m, κ_f, and κ_m are the Poisson ratios, shear moduli, and bulk moduli of the inclusion and matrix respectively.

The axial shear modulus, μ_{12}, was derived as a function of the concentration, c, and the independent shear moduli of the matrix and inclusion phases μ_m and μ_f:

$$\frac{\mu_{12}}{\mu_m} = \frac{\mu_f(1+c) + \mu_m(1-c)}{\mu_f(1-c) + \mu_m(1+c)} \qquad (2)$$

Finally, the transverse shear modulus, μ_{23}, was obtained from the solutions of a quadratic equation:

$$A\left(\frac{\mu_{23}}{\mu_m}\right)^2 + 2B\left(\frac{\mu_{23}}{\mu_m}\right) + C = 0 \qquad (3)$$

where the coefficients A, B, and C are algebraic expressions given in Christensen (1990).

To apply this model to dentin, we assumed that the tubule lumen with its surrounding, coaxial peritubular cuff could be modeled as a cylindrical inclusion with a Young's modulus, E_f, given by:

$$E_f = E_{pt}\left(1 - \frac{A_l}{A_{pt} + A_l}\right) \qquad (4)$$

where A_l is the lumen area, and E_{pt} and A_{pt} are the Young's modulus and area of the peritubular dentin. From the assumption that the constituent phases (intertubular matrix and peritubular dentin) are elastically isotropic, the values for the shear, μ_m, and bulk, k_m, moduli of the matrix phase were determined from the measured Young's modulus of the matrix phase from the relations:

$$\mu_m = \frac{E_m}{2(1+\nu_m)}$$

$$k_m = \frac{E_m}{3(1-2\nu_m)} \qquad (5)$$

where k_m is the bulk modulus of the matrix phase. Similar expressions apply for μ_f and k_f as well. From the above relationships (given in complete form in Christensen 1990), all of

dentin's continuum elastic properties could be described in terms of three measurable parameters: *c, E_m, and E_{pt}*.

specimen preparation

Six partially erupted human third molars with no visible or radiographic evidence of caries were used for this study. Thin (1 mm) transverse slabs through the mid–coronal dentin were cut from each tooth with a slow speed diamond saw (Isomet, Buehler) under constant irrigation. The slabs were assigned randomly to one of two groups (n=3). For Group 1, cubes of 1–mm side length were prepared with the tubules intersecting the superior and inferior cube faces and running parallel with the lateral cube faces (see Figure 1). Group 2 specimens were left as slabs. The specimens were polished in stages through 0.05 μm diamond and then rinsed in water and ultrasonicated to remove the smear layer. After rinsing, the specimens were allowed to dry in air up to seven days until AFM indentation was performed.

AFM indentation

The specimens were imaged and indented using a specially modified atomic force microscope (Nanoscope III, Digital Instruments, Santa Barbara, CA). The modification consisted of replacing the AFM cantilever/tip assembly with a transducer driven head and tip (Triboscope, Hysitron, Minneapolis, MN) that allowed the AFM to operate both as an imaging and an indentation instrument. This modification has been described in detail elsewhere [Balooch, et al. 1998].

The AFM was used initially to image the specimen, and sites were selected for indentation. The AFM tip was then brought in contact with the surface and the force on the tip was ramped linearly to between 400–700 micro Newtons, depending on whether indentations were made in intertubular or peritubular dentin (an attempt was made to keep the indentation depth constant, so as to minimize tip area errors). This maximum force was

held constant for a brief time interval, and was then decreased linearly to zero. The time increments were two seconds for each segment of the loading profile (see Figure 2a). The load displacement profile for a typical specimen is shown in Figure 2b. A polynomial expression, P_u, for the unloading curve was obtained from a least squares fit of the data between 20% and 95% of the maximum force:

$$P_u = B\left(h - h_f\right)^m \qquad (6)$$

where h was the indentation depth, h_f was the indention depth at zero force, and B and m were determined from a least squares fit of the unloading data. The derivative of the unloading curve evaluated at the peak force provided the contact stiffness, S[Oliver and Pharr, 1992]

$$S = \frac{dP_u}{dh}\bigg|_{h \to h_{\max}} = mB\left(h_{\max} - h_f\right)^{m-1} \qquad (7)$$

Care was taken to remove the uncalibrated machine compliance, C_m, which was associated with the tip shaft and sample mounting from each indentation:

$$S_c = \frac{1}{\left[(1/S) - C_m\right]} \qquad (8)$$

and C_m was determined by comparing compliance data for indentations at different depths [Kinney, et al., 1996].

The indentation modulus, E^*, was determined from the measured contact stiffness, S_c, and the contact areas for each indentation, A, that were obtained from the contact depth and the diamond–tip shape calibration [Doerner and Nix, 1986]:

$$E^* = \frac{\sqrt{\pi}}{2\sqrt{A}} S_c \qquad (9)$$

The Young's modulus of the probed specimen, E_s, was then obtained from E^* and the known modulus of the diamond indenter, E_i:

$$\frac{1}{E^*} = \frac{\left(1-\nu_s^2\right)}{E_s} + \frac{\left(1-\nu_i^2\right)}{E_i} \qquad (10)$$

The intertubular dentin in the Group 1 specimens was indented at 5 μm intervals approximately 100 μm inwards from the cube edge in a direction parallel with the tubule axis. The specimens were then rotated 90^o and indented along the direction normal to the tubule axis. Care was taken to make indentations in the same region of dentin to test for material anisotropy. Because these measurements required frequent repositioning of the specimen, it was difficult to fully immerse the cubes in water. Therefore, the cubes were indented dry for this part of the investigation.

The Group 2 specimens were indented in a direction parallel with the tubule axis, starting with dry specimens and then full water immersion with measurements at a half, two, 24, and 72 hours in water. The purpose of the repeated measurements was to study the effects of hydration on the modulus of dentin. Intertubular dentin was indented at a location midway between adjacent tubules, and peritubular dentin was indented across the full width of the cuff, as shown in Figure 3. Indentations were made across the full width of the cuff in order to measure the magnitude of boundary effects on the indentation modulus of the peritubular dentin. The precise location of each indentation was determined by AFM imaging. Measurements were repeated three times on each specimen.

Results

AFM indentation moduli across the width of a representative peritubular cuff are shown in Figure 4. Within a tenth of a micrometer of both the lumen wall and the intertubular dentin interface, the modulus was noticeably reduced by boundary effects. However, across the bulk of the peritubular cuff, remarkably constant values were obtained. The peritubular modulus was 28.6±.5 GPa, and was rounded to 30 GPa for E_{pt} in Equation 4 so as not to underestimate the mechanical contribution of the tubules. The values for A_l and A_{pt} as a function of location in the tooth are listed in Table 2, based on tubule areas calculated by Pashley [1989] from the data of Garberoglio and Brannstrom [1976]. Substituting these values into Equation 4 produced an inclusion modulus, E_f, that was independent of position (22.5 GPa).

The intertubular modulus was measured in two orientations: perpendicular with the tubule axis and parallel with the axis. Measurements perpendicular to the tubule axis gave values of 20.1±1.1 GPa and those made parallel with the axis were 20.3±.9 GPa. There was no statistically significant effect of orientation on the measured values of the peritubular and intertubular dentin moduli based on a two–tailed T test ($p>.7$).

The modulus of the intertubular dentin as a function of time in water is graphed in Figure 5. There was a rapid decrease in elastic modulus in the first 24 hours, followed by a more gradual decrease over the next 48 hours. Concerns about possible specimen demineralization led us to select the 24 hour time point (E_m = 15 GPa) for modeling purposes (see discussion).

With the values of E_m and E_f, the five independent elastic constants were determined as a function of tubule concentration. Because there were no independent measures of Poisson's ratio, three limiting cases were explored: $\nu_m < \nu_f$; $\nu_m = \nu_f$; $\nu_m > \nu_f$, where ν_f was given a constant value of 0.25 and ν_m ranged from 0.1 to 0.4. The magnitudes of the axial Young's modulus and axial and transverse shear moduli are charted as a function of tubule concentration in Figure 6. All moduli increased linearly with tubule concentration as

expected. The axial Young's modulus increased from about 15.3 GPa near the dentin enamel junction to 16.3 GPa within a mm of the pulp. There was only a slight effect of varying Poisson's ratio. The effects of Poisson's ratio were more pronounced on the magnitudes of the shear moduli, a natural consequence of Equation 5. At 10% tubule density, the axial and transverse shear moduli ranged from about 5.5 to 7 GPa as Poisson's ratio of the intertubular matrix was varied from 0.1 to 0.4. The axial and transverse shear moduli were identical over the expected range of tubule concentration in healthy dentin.

Discussion

The micromechanics model developed here operates at the composite level, accounting for the interaction of the continuous matrix phase with an inclusion phase, in this case the hypermineralized peritubular cuffs. If the materials properties of the two phases are known, then a micromechanics model can be used to predict the effective properties of the composite material. Strictly speaking, a micromechanics model applies to a statistically homogeneous material. The tubule density of dentin, however, varies slightly from the dentin enamel junction towards the pulp. However, the variations in tubule density are small enough that we can define a representative volume element that is large compared with the tubule diameters and spacing, and over which the calculated effective properties correctly define the relations between the field variables of stress and strain.

There are as yet no constitutive models that describe the mechanical behavior of the dentin matrix as a function of mineralization and fiber orientation, nor is the organization of the dentin matrix fully understood. Nevertheless, it is possible to measure a Young's modulus of the matrix (intertubular dentin) and peritubular dentin with atomic force indentation. These values can be used in a micromechanics model to predict the effective properties of dentin, perhaps more accurately than they can be measured with conventional biomechanical testing since physical measurement of bulk dentin properties is so difficult.

In a previous study of human dentin, we reported a Young's modulus of intertubular dentin that ranged from 17.7–21.1 GPa and for peritubular dentin of 29.8 GPa [Kinney, et al., 1996]. These measurements were made with a Nanoindenter™, which could not operate under water. Also, because the Nanoindenter is not an imaging device, it was impossible to know with certainty where the indentations were made with respect to the dentin microstructure. Therefore, the reported values for the intertubular dentin were considered to be upper bounds, and the value for the peritubular dentin was considered to be a slightly lower estimate because of possible influence of the intertubular dentin or the tubule lumen. With the atomic force microscope used in this study, the precise location of each indentation could be recorded and the indentations could be made with the specimens fully immersed in water. It was not surprising to find the AFM measurements of the intertubular modulus significantly lower than previously reported. It is also important to note that the AFM indentations of the peritubular dentin gave modulus values that were in close agreement with previous work [Kinney, et al. 1996]. This is because peritubular dentin has very low organic content and is not appreciably affected by drying.

The effects of hydration on the mechanical properties of mineralized tissues has been previously reported. In the first systematic study of this effect, Currey reported that three hours of rehydration was sufficient to restore the elastic modulus of dried specimens to their original value [Currey, 1988]. In addition, Jameson, et al. (1993) determined that the stress and strain at fracture could be restored to original values after 96 hours of rehydration in deionized water. Although the time points used in our study were too widely separated to confirm that three hours proposed by Currey was sufficient to restore the elastic properties of the dentin, we did not observe any significant change in modulus after 24 hours of rehydration. However, there was a trend towards a slight decrease between 24 and 72 hours. We were concerned that this continued decrease might have been a result of surface demineralization in water, an affect that has been observed by others in mechanical test

specimens of bone [Gustafson, et al. 1996]. To mitigate this possibility, we chose to use the 24 hour time point for evaluating the Young's modulus of the intertubular dentin.

Tubule number density increases from about 4 vol% near the dentin enamel junction to about 16 vol% within one mm of the pulp [Garberoglio and Branstrom, 1976; Pashley, 1989]. Although the number density of tubules increase with depth and should therefore increase the effective modulus, any increase is partially offset by the corresponding decrease in the volume fraction of the matrix phase. Therefore, over this range in density, the tubules have only a slight affect on the magnitude of the elastic constants. Furthermore, Poisson's ratio of the matrix phase affects only the magnitude of the shear moduli, and has only a negligible affect on the axial Young's modulus.

The model makes three predictions. First, the model predicts that in healthy, primary coronal dentin there is a slight increase in the elastic modulus subjacent to the mantel inwards. Second, the model predicts that the properties of the matrix dominate the mechanical behavior of the bulk dentin. Finally, the model predicts that the axial and transverse shear moduli are the same regardless of Poisson's ratio.

The largest uncertainty in the present study is the magnitude of the shear modulus. We are aware of only one attempt to measure the shear modulus [Renson and Braden 1975]. These investigators obtained a shear modulus of 6.1 GPa in torsion, and made the observation that there was no apparent effect of tubule orientation on their results, although there was no way to precisely control tubule orientation in the macroscopic dentin beams used in their study. The magnitude of their shear modulus was consistent with a Poisson's ratio near 0.25. Indeed, for those specimens for which both the Young's and shear modulus were measured, Renson and Braden obtained a mean Poisson's ratio of 0.23.

The most critical assumptions in the proposed micromechanics model are that the matrix phase is homogeneous and isotropic. Previous studies have shown that in primary dentin the mineralization is uniform at about 40–45 vol%, and that measurable deviations from this value occur only in the immediate vicinity of the dentin enamel junction (mantle

dentin) or the pulp [Kinney, et al., 1994]. Therefore, by confining our model to primary dentin, we were reasonably assured of mineral homogeneity. The assumption of elastic isotropy, however, requires careful consideration. Dentin's microstructure, both from the orientation of the tubules as well as the planar confinement of the collagen fibrils perpendicular to the tubules, gives the appearance of orthotropic symmetry. However, there is no compelling evidence that dentin's elastic properties are anisotropic. Furthermore, our AFM indentations detected no anisotropy in the Young's modulus when measured in orthogonal directions. However, it has recently been observed that the transverse shear strength may be greater than the axial shear strength [Watanabe et al., 1996]. It is possible for the dentin matrix to be elastically isotropic yet have an orientation dependence of shear strength from the presence of the tubule lumens acting to increase the energy required to propagate a crack in the transverse direction. The question of elastic isotropy will only be resolved by careful measurement of the elastic modulus as a function of tubule orientation.

In summary, our results predict that the intertubular dentin matrix governs the elastic behavior of dentin, and that the tubules do not introduce elastic anisotropy. Combining the indentation data on the intertubular and peritubular dentin with the cylindrical inclusion micromechanics model gave the values for the five independent elastic constants that are listed in Table 3. Until better indentation or shear moduli data become available, primary dentin should be modeled as an isotropic material with these values of the elastic constants.

Acknowledgments

This work was funded by the U.S. National Institutes of Health, NIDCR under grant number PO1DE09859. The authors wish to thank Prof. R.M. Christensen for valuable discussions. The work was performed under the auspices of the U.S. Department of Energy, Lawrence Livermore National Laboratory, contract W–7405–ENG–48. We thank L. Watanabe (U.C. San Francisco) and R. Kershaw (Lawrence Livermore National Laboratory) for sample preparation.

References

Balooch M., Wu–Magidi I.C., Balazs A., Lundkvist A.S., Marshall S.J., Marshall G.W., Siekhaus W.J., and Kinney J.H. (1998) Viscoelastic properties of demineralized human dentin measured in water with atomic force microscope–based indentation. J. Biomed. Mater. Res. **40**,539–544.

Bowen R.L. and Rodriguez M.M. (1962) Tensile strength and modulus of elasticity of tooth structure and several restorative materials. J.Am. dent. Ass. **64**,378–387.

Christensen R.M. (1990) A critical evaluation for a class of micromechanics models. J. Mech. Phys. Solids **38**:379–404.

Craig R.G. and Peyton F.A. (1958) Elastic and mechanical properties of human dentin. J. dent. Res. **37**,710–718.

Currey J.D. (1988) The effects of drying and rewetting on some mechanical properties of cortical bone. J Biomech. **21**,439–441.

Doerner M.F. and Nix W.D. (1986) A method for interpreting the data from depth–sensing indentation instruments. J Mater. Res. **1**, 601–609.

Garberoglio R. and Brannstrom M. (1976) Scanning electron microscopy investigation of human dentinal tubules. Arch oral Biol. **21**,355–362.

Gustafson M.B., Martin R.B., Gibson V., Storms D.H., Stover S.M., Gibeling J., and Griffin L. (1996) Calcium buffering is required to maintain bone stiffness in saline solution. J. Biomech. **29**,1191–1194.

Haines D.J. (1968) Physical properties of human tooth enamel and enamel sheath material under load. J.Biomech. **1**,117–128.

Hashin Z. (1983) Analysis of composite materials–A survey. J. appl. Mech. **50**,481–503.

Huang T–J. G., Schilder H and Nathanson D (1992) Effects of moisture content and endodontic treatment on some mechanical properties of human dentin. J Endodontics **18**,209–215.

Jameson M.W., Hood J.A.A., and Tidmarsh B.G. (1993) The effects of dehydration and rehydration on some mechanical properties of human dentine. J. Biomech. **26**,1055–1065.

Katz J.L. (1971) Hard tissue as a composite material–I. Bounds on the elastic behavior. J. Biomech. **4**,455–475.

Kinney J.H., Marshall G.W., and Marshall S.J. (1994) Three–dimensional mapping of mineral densities in carious dentin: theory and method. Scanning Microsc. **8**,197–204.

Kinney J.H., Balooch M., Marshall S.J., Marshall G.W., and Weihs T.P. (1996) Hardness and Young's modulus of peritubular and intertubular dentine. Arc. oral Biol. **41**,9–13.

Lehman M.L. (1967) Tensile strength of human dentin. J. dent. Res. **46**,197–201.

Marshall G.W. (1993) Dentin: Microstructure and characterization. Quintessence Int. **24**,606–617.

Meridith N., Sherriff M., Setchell D.J. and Swanson S.A. (1996) Measurement of the microhardness and Young's modulus of human enamel and dentine using an indentation technique. Archs. oral Biol. **41**,539–545.

Neumann H.H. and Di Salvo N.A. (1957) Compression of teeth under the load of chewing. J. dent. Res. **36**, 286–290.

Oliver W.C. and Pharr G.M. (1992) An improved technique for determining hardness and elastic modulus using load and displacement sensing indentation experiments. J Mater. Res. **7**,1564–1583.

Pashley D.A. (1989) Dentin: A dynamic substrate–A review. Scan. Microsc. **3**,161–176.

Peyton F.A., Mahler D.B. and Hershenov B. (1952) Physical properties of dentin. J. dent. Res. **31**,336–370.

Renson C.E. (1970) An experimental study of the physical properties of human dentine. Ph.D. Thesis, University of London.

Renson C.E. and Braden M. (1971) The experimental deformation of dentine by indenters. Archs oral Biol. **16**,563–572.

Renson C.E. and Braden M. (1975) Experimental determination of the rigidity modulus, Poisson's ratio and elastic limit in shear of human dentine. Archs oral Biol. **20**,43–47.

Rees J.S., Jacobsen P.H., and Hickman J. (1994) The elastic modulus of dentine determined by static and dynamic methods. Clin Mater. **17**,11–15.

Sano H., Ciucchi B., Matthews W.G., and Pashley D.H. (1994) Tensile properties of mineralized and demineralized human and bovine dentin. J Dent Res **73**:1205–1211.

Stanford J.W., Paffenbarger G.C., Kumpula J.W. and Sweeney W.T. (1958) Determination of some compressive properties of human enamel and dentin. J. Am. Dent. Ass. **57**,487–495.

Stanford J.W., Weigel K.V., Paffenbarger G.C. and Sweeney W.T. (1960) Compressive properties of hard tooth tissue and some restorative materials. J.Am. Dent. Ass. **60**,746–756.

Ten Cate A.R. (1994) Oral Histology: Development, Structure, and Function, 4th Edition. Mosby Book Co., St. Louis.

Tyldesley W.R. (1959) The mechanical properties of human enamel and dentine. Br. dent. J. **106**,269–278.

Watanabe L., Marshall G.W., and Marshall S.J., (1996) Dentin shear strength: Effects of tubule orientation and intra–tooth location. Dent. Mater. **12**,109–115.

Watts D.C., El Mowafy O.M., and Grant A.A. (1987) Temperature dependence of compressive properties of human dentin. J. dent. Res. **66**,29–32.

Xu H.H.K., Smith D.T., Jahanmir S., Romberg E., Kelly J.R., Thompson V.P. and Rekow E.D. (1998) Indentation damage and mechanical properties of human enamel and dentin. J. dent. Res. **77**,472–480.

Tables

Table 1: Reported values of the Young's modulus of dentin

Authors and date	Method	Young's Modulus (GPa)
Peyton et al. (1952)	compression	11.6
Neumann and Di Salvo (1957)	compression	1.6–11.7
Craig and Peyton (1958)	compression	18.3
Stanford et al. (1958)	compression	11.0
Tyldesley (1959)	4–point bending	12.3
Stanford et al. (1960)	compression	11.7–13.8
Bowen and Rodriguez (1962)	tension	19.3
Lehman (1967)	tension	11.0
Haines (1968)	compression	11.0
Renson (1970)	compression	12.8
Renson (1970)	cantilever bending	12.0
Renson and Braden (1971)	indenter	12.0
Renson and Braden (1975)	cantilever bending	11.1–19.3
Watts, et al. (1987)	Compression	13.9±1.5 (25C)
Huang et al. (1992)	Compression	14.9
Van Meerbeek (1993)	Nanoindenter	19.3
Sano (1994)	tensile	13–15
Rees et al. (1994)	3–point bending	8.6 (s):14.3–15.8 (d)*
Meridith, et al. 1996	Indentation	8.7–11.2
Xu et al. (1998)	Indentation	20.3 ± 1.7

* (s) = static modulus; (d) = dynamic modulus

Table 2: the elastic modulus of the cylindrical inclusion (lumen+peritubular cuff) with position (based on values from Garberoglio and Brannstrom (1976) as tabulated by Pashley (1989)).

Distance from pulp (mm)	**A_l**	**A_p**	**A_i**	**E_f (GPa)**
1.1–1.5	4.0	11.9	84.1	22.5
1.6–2.0	2.9	8.6	88.5	22.5
2.1–2.5	1.5	4.4	94.1	22.5
2.6–3.0	1.0	3.0	96.0	22.5
3.1–3.5	1.0	2.9	96.1	22.5

Table 3: Model predictions for the five independent elastic constants of dentin assuming Poisson's ratio of .25 for peritubular and intertubular dentin.

Location	E_{11} (GPa)	μ_{12} (GPa)	μ_{23} (GPa)	K_{23} (GPa)	ν_{12}
Inner dentin	16.1–16.4	6.3–6.4	6.3–6.4	12.7–12.9	.25
Outer dentin	15.3–15.6	6.1–6.2	6.1–6.2	12.4–12.5	.25

List of Figures

Figure 1:

Photomicrograph of a 1–mm cube dentin. The locations of the indentations, both parallel and perpendicular to the tubule axis, are circled. The arrow lies in the approximate direction of the tubules.

Figure 2a:

The force applied to the indenter tip as a function of time. The load cycle consisted of three, 2–second segments: a linear ramp, a constant hold, and a linear decrease.

Figure 2b:

A typical force/displacement profile for indentation in intertubular dentin.

Figure 3:

Artist rendering of the hypermineralized peritubular cuff showing the approximate locations of the indentations.

Figure 4:

Young's modulus of peritubular dentin measured as a function of radial distance from the lumen wall. Within 0.1 micrometer of the lumen and the peri–intertubular dentin interface, the Young's modulus is much lower due to interaction with the boundaries. Within the bulk of the peritubular dentin, the measured values vary by less than 2% of the mean value of 28.6 GPa.

Figure 5:

The Young's modulus of intertubular dentin as a function of time in water, starting from the dry state at time zero.

Figure 6: a) axial Young's modulus as a function of tubule concentration for three values of the Poisson's ratio of the intertubular dentin matrix. b) axial shear modulus as a function of tubule concentration for three values of the shear modulus. c) transverse shear modulus of dentin. d) the ratio of the axial to transverse shear moduli in dentin. The apparent discontinuities in the graph (6d) are a result of round off error in calculating the ratios to two significant figures. Over the entire range of tubule concentration the two shear moduli differ by less than 1%.

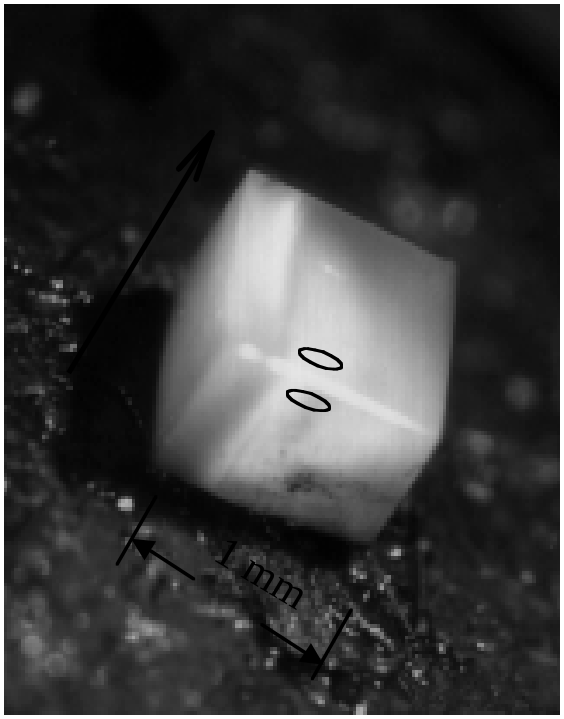

Kinney, et al. Figure 1

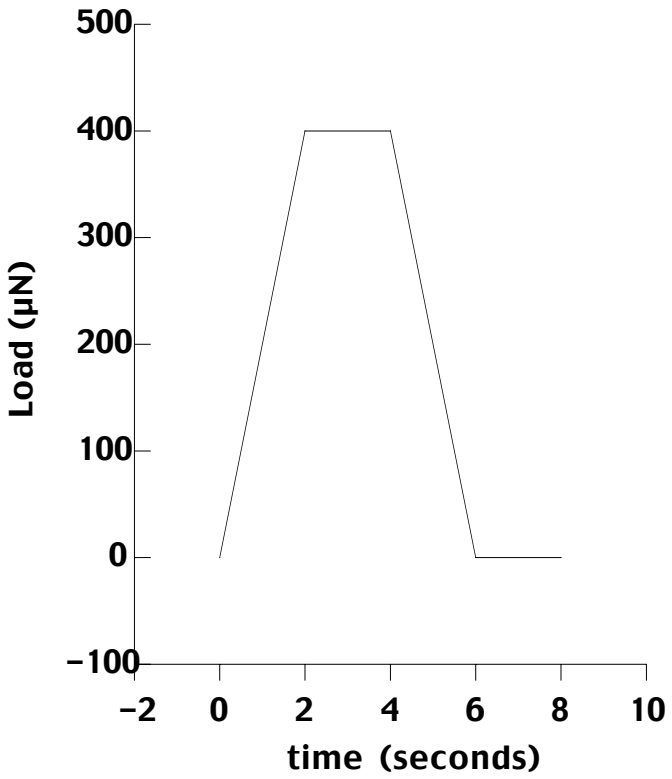

Kinney, et al. Figure 2 a

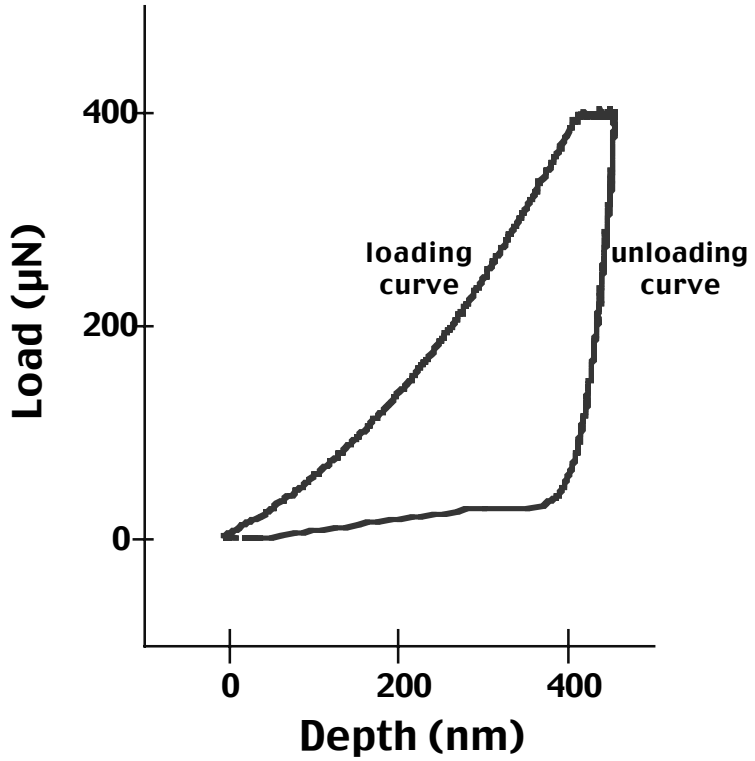

Kinney, et al. Figure

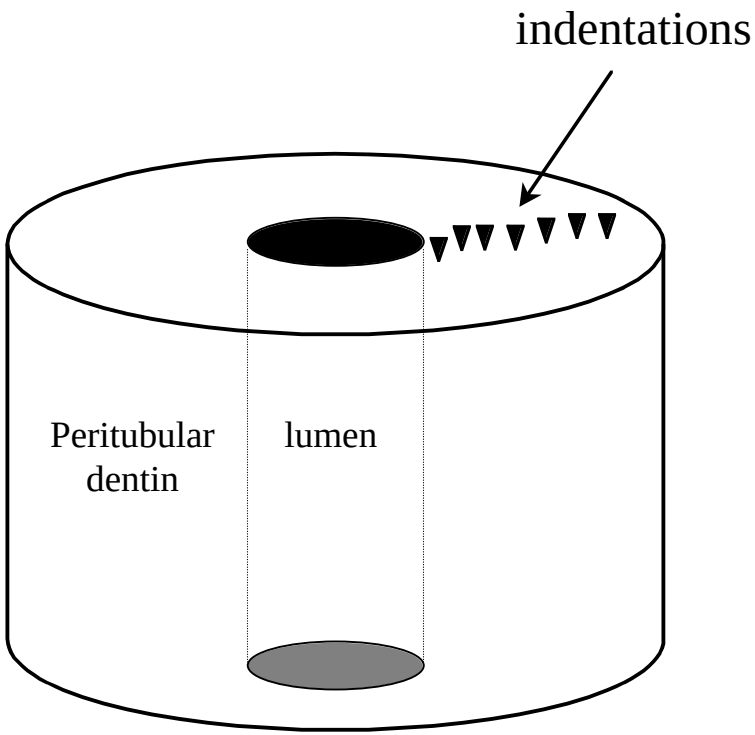

Kinney, et al. Figure 3

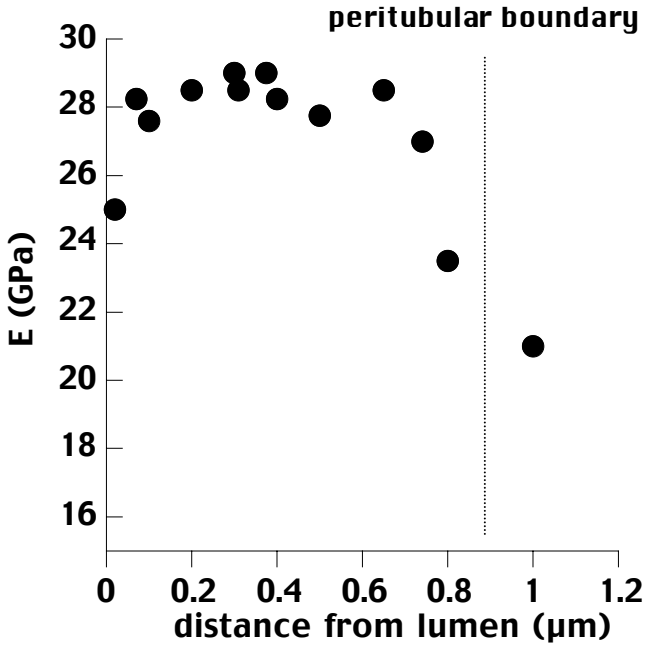

Kinney, et al. Figure 4

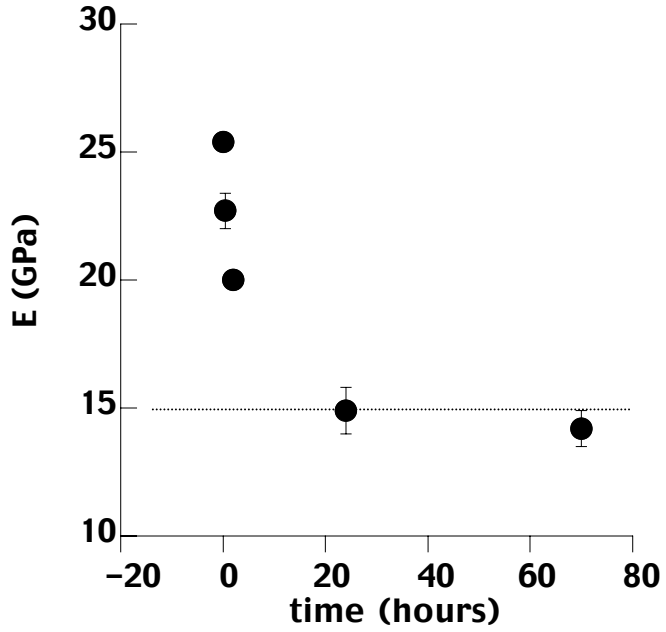

Kinney, et al. Figure 5

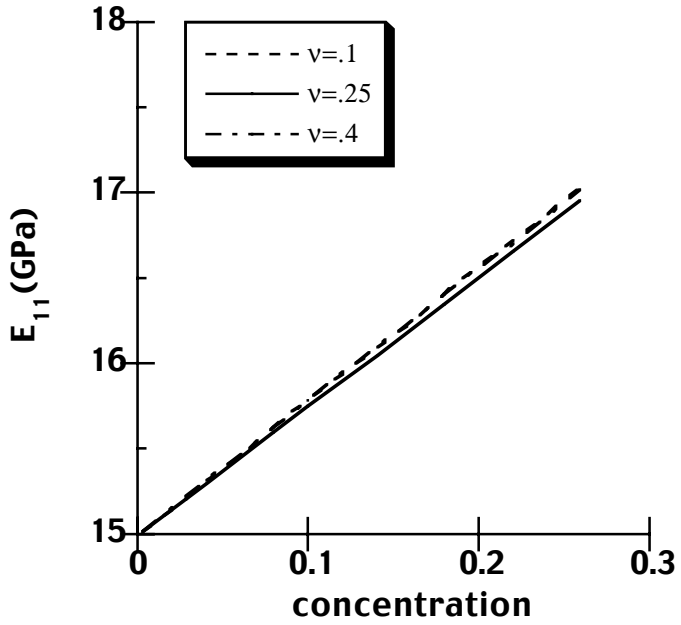

Kinney, et al. Figure 6a

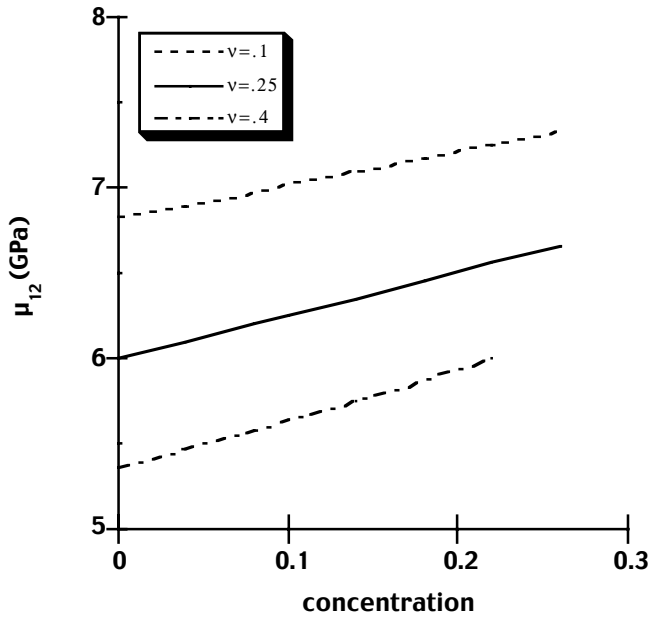

Kinney, et al. Figure 6b

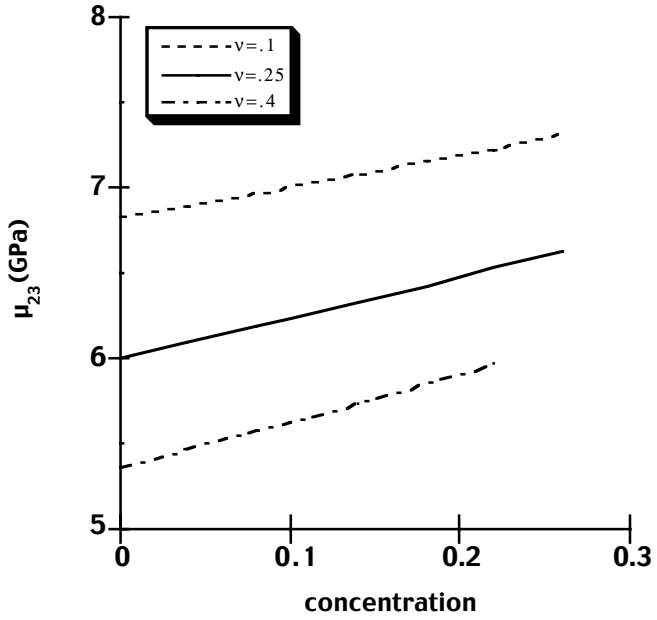

Kinney, et al. Figure 6c

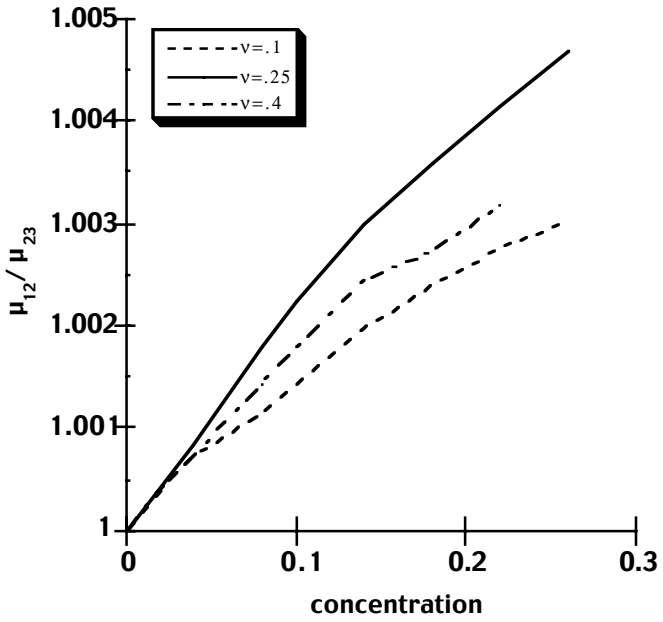

Kinney, et al. Figure 6d